High torque, low velocity pneumatic rotary servomotor

International Journal of Applied Engineering Research ISSN 0973-4562 Volume 11, Number 19 (2016) pp. 9914-9920

High torque, low velocity pneumatic rotary servomotor

Stefano Mauro, Giuliana Mattiazzo and Massimo Sorli

Politecnico di Torino, Department of Mechanical and Aerospace Engineering, Italy.

Abstract
The work deals about the design of a pneumatic rotating servomotor intended for low speed, high torque operation. The servosystem is based on a pneumatic orbital motor working in the 0 – 80 rpm range with a maximum torque of 28 Nm, and hence it can be applied in heavy duty application. The paper analyses the kinematic layout of the motor, shows the results of characterisation tests and finally it discusses the layout and the components to implement closed loop velocity control. The effectiveness of control layout based on the use of pressure proportional and flow proportional valves is compared by experimental tests. The results show the capabilityof the servosystem to keep the set velocity and to react to external disturbance.

Keywords: Pneumatic servosystem, pressure proportional valve, rotary motor

INTRODUCTION

A large number of applications requires velocity controlled servoactuators, which, in general, can be based on electric, hydraulic or, less often, pneumatic motors. The technology is chosen on the basis of the application requirements, such as maximum velocity, torque or force, accuracy, frequency response and power/mass ratio. Economic consideration, which include procurement, installation and maintenance costs, must also be considered in the design phase. In general when high force or torque and low mass are required, hydraulic technology is applied. Electric servomotors, on the contrary, benefit of easiness of installation, as they do not require pumping unit and supply pipelines, and ensure large bandwidth. However the power/mass ratio is lower than in hydraulic system, and so they are not the best solution when the needed torque or force are high and mass is a critical design parameter.

Pneumatic technology can constitute an intermediate solution to be applied in those cases in which relatively high forces or torques are required, while requirements about readiness of the servosystem and bandwidth are not so demanding. In those cases, in fact, the mass and cost increase related with the use of electric solutions or the construction of hydraulic power source and heavy piping is not justified. Examples of possible application are not only in the industrial and automation fields: for instance, parallel architecture machines used to move relatively large loads, as in some sun tracker or motion simulation systems [1-5] can be conveniently powered by pneumatic servosystems. Some application can be found also in the biomedical field [6-7], in road and rail vehicles [8-9], etc. All the technologies show sensitivity to environmental condition and control parameter [10-14].

A number of authors faced the problem of developing pneumatic servosystems with relevant performance. Lee, Yao and Shang [15-17] analyse the results that can be obtained with adaptive control. Donell, Mattiazzo and Nunez [18-20] show application of pneumatic servoaxis to robots, while Comber [21] describes an application in the field of robotics for surgery.

Within the present work the design and test of a pneumatic rotary servosystem based on an orbital pneumatic motor is analysed. The servosystem is intended for medium load application, with a torque up to 28 Nm and velocity ranging from 0 to 80 rpm. The paper considers both the application of a pressure proportional valve and of flow proportional valves based on modulating digital valves. The paper describes the control algorithm that were developed for both the solution and show the experimental results.

SYSTEM DESCRIPTION

Figure 1 provides a schematics of the orbital pneumatic motor used to develop the servosystem.

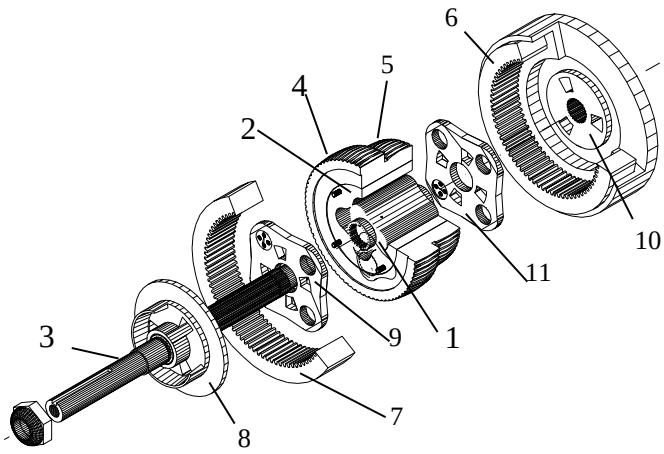

Figure 1: Orbital pneumatic motor schematics

The compressed air expands in the chambers composed by the intersections of the teeth and caves of the two cycloidal gears 1 and 2. The inner gear 1 has three teeth and it is co-axial with the output shaft 3. Gear 2 has four teeth and its axis is eccentric with respect to that of gear 1, so that variable volume chamber constitute during the relative motion of the gears, according to a technique currently used for hydraulic motors. A two stages epicycloidal reducer composed by gears 4,5,6, and 7 transmits motion from the axis of gear 2 to the

output shaft 3 with a reduction ratio equal to 96.2. This high value of transmission ratio involves that the torque disposable at the output shaft can be very high at low rotating speeds.
Air distribution is controlled by the two couples of rotating plates 8,9 and 10,11. Each couple is composed by a plate with three holes (8,10) and by one with four holes (9,11). Plates 8 and 10 rotates with the output shaft 3, while plates 9 and 11 are fixed to gear 2. In order to ensure a correct distribution, plate 8 is assembled with 90° rotation with respect to plates 10, and plates 9 and 11 show a 45° relative rotation. The overlapping of the holes in the plates depends on the relative position of the shaft and of the cycloidal gear, and it determines the opening laws of inlet and exhaust ports.

TEST SET-UP

The tested motor was assembled within the test circuit showed in Figure 2.
The output shaft of the motor (1) is fixed to torquemeter (2) by means of the flexible joint (3). The output shaft of the torquemeter is connected through flexible joint (4) to a magnetic powder brake (5) which provides a controlled resisting torque. A tachometric sensor build inside the torque measurement equipment provides a rotating speed signal which is used for feedback and measurement.

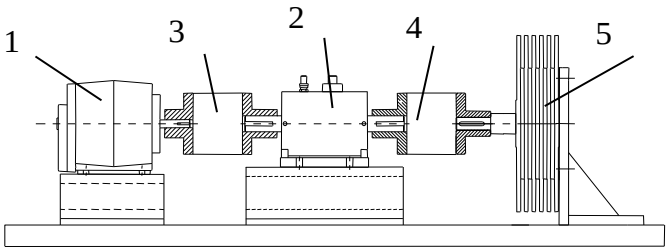

Figure 2: Test set up

Figure 3 shows the pneumatic circuit with proportional valve.

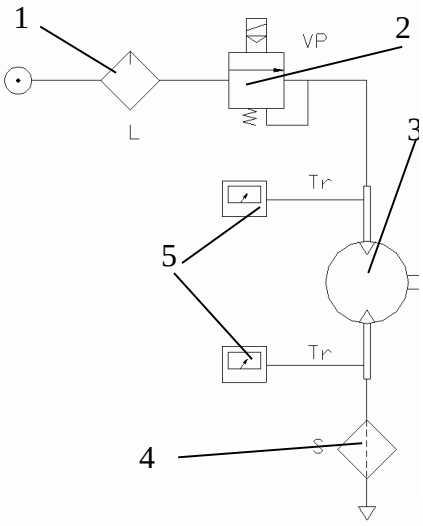

Figure 3: Pneumatic circuit with pressure proportional valve

The compressed air is suitably lubricated by lubricator (1), then a pressure proportional valve (2) rules the supply pressure for motor (3). Finally the air is exhausted through filter (4). The ports of the motor are equipped with ISO pipes and pressure transducers (5) in order to measure the actual supply and exhaust pressure. The pressure proportional valve is the well known Parker P3P-R with maximum ruled pressure of 10 bar and maximum flow rates of 200 Nl/s ANR. Fig. 4 reports its Bode diagram as provided by the manufacturer. The analysis of the static and dynamic performance of that valve was presented by Sorli et al. in [22].

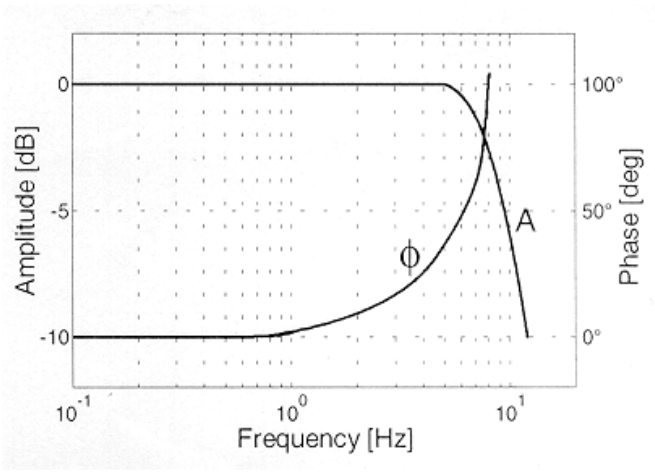

Figure 4: Bode Diagram of the Lucifer valve

Figure 5 shows the circuit layout with modulating digital valves. In this case valves are driven according to PWM modulation technique.

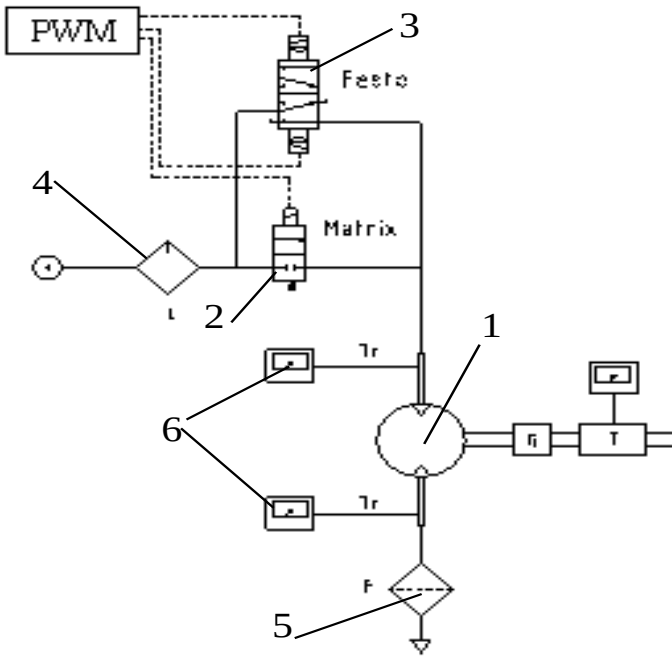

Figure 5: Pneumatic circuit with digital valves

In that case the compressor supplies the motor (1) through a couple of digital valves 2 and 3. The lubricator (4), the filter (5) and the pressure transducers (6) are the same of the former case. Valve 2 is build by Matrix, type MX751.80BC224, with nominal flow rate of 800 Nl/min ANR at 7 bar, with cut-off frequency of 100 Hz. Valve 3 is build by FESTO, type JMFH-5-1/4, with nominal flow rate of 1600 Nl/min ANR at 7 bar and cut-off frequency lower than 15 Hz. In order to obtain a behaviour similar to that of a 2/2 valve some ports were closed. The supply flow rate is ruled by controlling the duty-cycle of pulse width modulation for valves 2 and 3. According to their different dynamic performance, the Matrix valve is driven with a 50 Hz carrier frequency, while this value is fixed at 8 Hz for the Festo valve, according to a technique analysed in [23].

MOTOR CHARACTERISATION TESTS

A large number of tests was carried out in order to measure the mechanical characteristic of the motor. The provided torque vs. shaft velocity characteristic was measured for different values of pressure drop across the motor. Under the same conditions the total flow rate was measured by combining the filter flow characteristics and the direct measure of its upstream pressure. These data are useful for the validation of a model and they allow the measurement of the efficiency. Fig. from 6 to 8 report the mechanical characteristic at constant pressure drop, the measured flow rate and the efficiency, respectively.

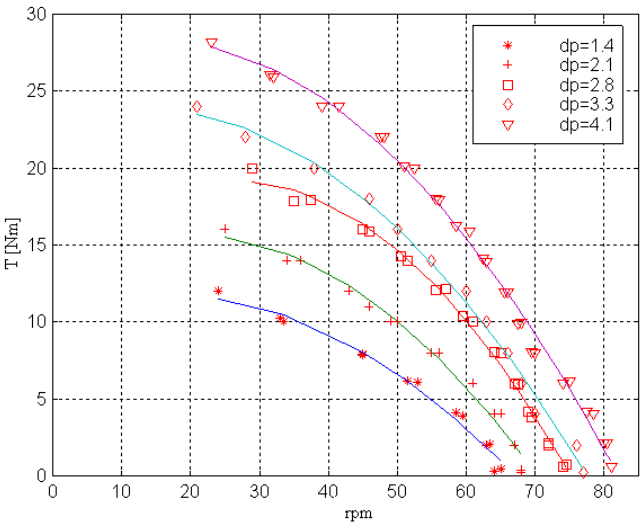

Figure 6: Mechanical characteristic at constant pressure drop

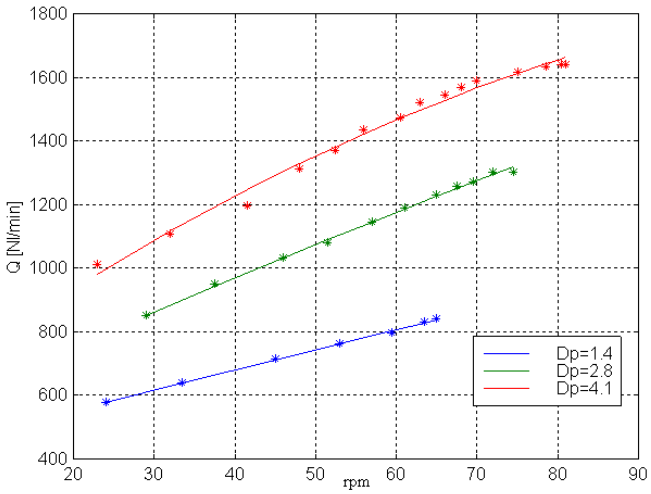

Figure 7: Flow rate

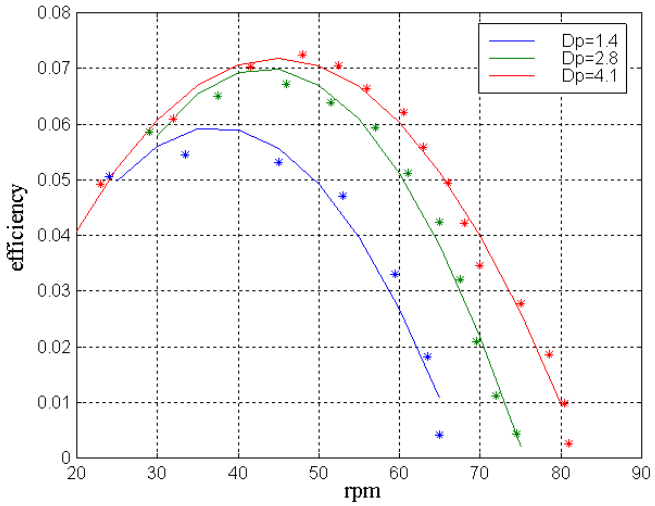

Figure 8: Efficiency

CONTROL WITH PRESSURE PROPORTIONAL VALVE

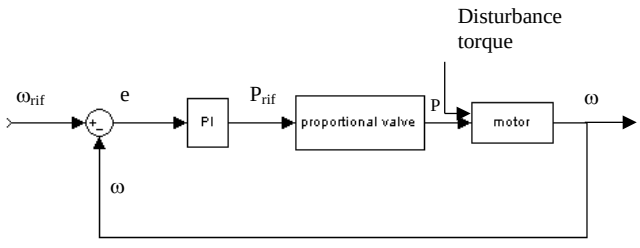

Figure 9: PI control schematics with pressure proportional valve

In a first attempt, the control was carried out implementing a simple PI controller, according to the schematics of Fig. 9. The velocity error is compensated by a PI controller in order to generate a pressure reference for the proportional valve. This last component rules the actual supply pressure for the motor. The results obtained with this technique were not satisfactory, as because of the strong non linearity of the system it was not possible to identify a couple of gain values capable of giving good precision and response time in any working condition. It was then analysed the possibility of using a feed forward controller and that of applying integral and proportional gains linearly depending on the error absolute value according to

$$k_p = k_{p0} + k_{p1} \cdot |e| \quad (1)$$

$$k_i = k_{i0} + k_{i1} \cdot |e| \quad (2)$$

A number of trials and the analysis of the best gains found for different working conditions led to the definition of the parameter values listed below, which are suitable if the error is expressed in rad/s and the pressure signal for the valve in bar: $k_{p0} = 0.03 \quad k_{p1} = 0.02 \quad k_{i0} = 2 \quad k_{i1} = 0.02$

This solutions allows the best results to be obtained; Fig. 10 shows the response to different velocity reference steps starting from about 30 rpm and stepping to 40, 45, 50, 55, 60, 65 and 70 rpm with a constant resisting torque of 5 Nm. Fig. 11 shows the response to the introduction of a step torque disturbance raising from 5 to 20 Nm with a constant velocity reference of 50 rpm.

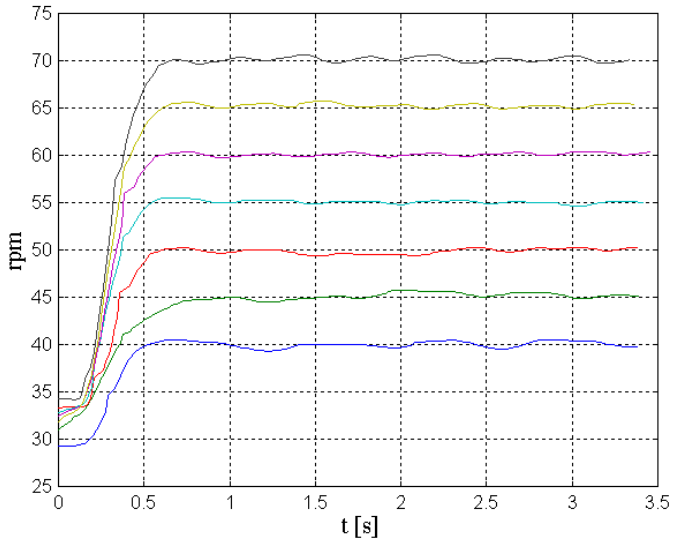

Figure 10: Step reference

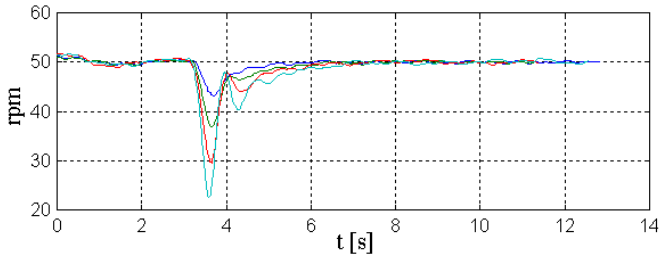

Figure 11: Response to a torque disturbance

The results show that the system response time to a step reference change is about 0,6 s, while effect of torque disturbance are recovered in 2.5 s. Precision in velocity tracking is affected by torque ripple and is in the ± 1 rpm range.

CONTROL WITH MODULATING DIGITAL VALVES

The need for high flow rate, up to 1800 Nl/min ANR, and very short response time is satisfied coupling a slow, large size valve (Festo) with a fast, small size one (Matrix). The Festo valve is supposed to ensure the larger part of the flow, while the Matrix valve should allow a fast change in the conductance in order to ensure a faster answer of the system. Fig. 12 shows the control schematics.

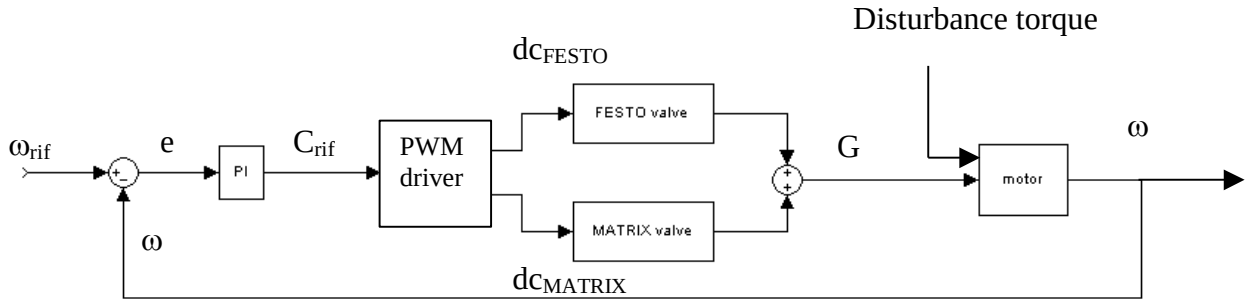

Figure 12: Control schematics with PWM driven digital valves

The angular velocity error is processed by a PI compensator which computes a conductance C_{rif} which should be ensured by the couple of PWM driven valves; the value is then processed by the PWM driver which generates the square wave command signal for the digital valves, ruling the mass flow rate directed to the motor.

According to the PWM flow control technique, the maximum update frequency for the command signal coincides with the carrier frequency of the modulation. In this application the carrier frequency for the Festo valve is fixed in 8 Hz, while the same value for the Matrix valve is fixed in 50 Hz. These values are selected combining the opposite needs for high frequency and narrow dead bands around zero and maximum. As it is evident, both the properties depend on the valve response time.

The total conductance of the couple of valves was experimentally measured for different values of their duty cycles. The tests were carried out on a test rig equipped with a diaphragm flow rate transducer. The couple of tested valves was assembled in parallel and supplied with constant pressure, while their downstream pressure was ruled by mean of a variable resistance. The flow rate was measured for different values of downstream pressure according to ISO 6853 and the conductance of the couple of valves was computed. The test was carried out considering different duty cycle values for both the valves. Fig. 13 shows the obtained results.

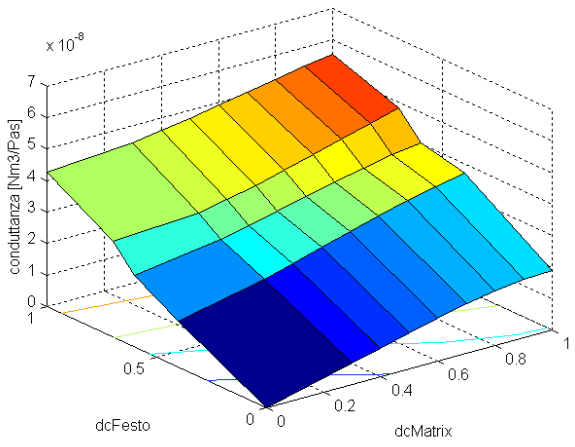

Figure 13: Conductance of the coupled valves

The results, though non linear, can be approximated by a plane in which the total conductance is computed as a linear combination of the duty cycles of the two valves.

$$C_{eq} = (a_1 dc_{Matrix} + a_2 dc_{Festo}) \qquad (3)$$

Using a minimum square algorithm, the best approximating plane was found to be defined by the following coefficients:

$$a_1 = 2 \cdot 10^{-8} \ \frac{\mathrm{Nm}^3}{\mathrm{sPa}} \ ; \ a_2 = 3.9 \cdot 10^{-8} \ \frac{\mathrm{Nm}^3}{\mathrm{sPa}}$$

A defined conductance value can be obtained with different couples of duty cycle values; a possible solution to choose one within all the possible couples of values is to impose them to lay on a straight line in the $dc_{Festo} - dc_{Matrix}$ plane, according to

$$b_1 dc_{Matrix} + b_2 dc_{Festo} + 1 = 0 \qquad (4)$$

After some experimental test, it was chosen the line defined by $b_1 = -3.7$; $b_2 = 1.7$ as it allows the duty cycle of the MATRIX valve to be kept far from the dead zone and the workspace of the FESTO valve to be completely used.

According to this choice, combining Eq. 4 with Eq. 3, the duty cycles to realise a desired conductance are then computed by

$$dc_{Festo} = \frac{C_{eq} + \frac{a_1}{b_2}}{a_2 - a_1 \frac{b_1}{b_2}} \ ; \ dc_{Matrix} = \frac{C_{eq} + \frac{a_2}{b_1}}{a_1 - a_2 \frac{b_2}{b_1}} \qquad (5)$$

A trial and error process lead to identify an optimal couple of proportional and integrative gains (kp = 0.01 C_{max}, ki = 0.08 C_{max})

Fig. 14 shows some results relative to the response to a step reference rising from 30 rpm to 40, 50 and 60 rpm respectively in presence of a resisting torque of 10 Nm. Fig. 15 reports the response to a torque disturbance of 10 Nm when the reference angular velocity is kept constant at 50 rpm.

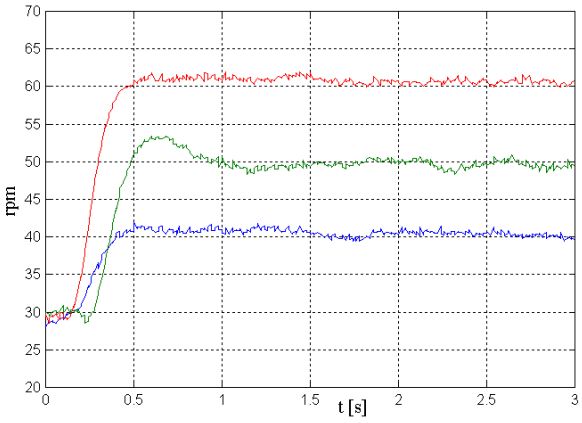

Figure 14: Response to a step reference

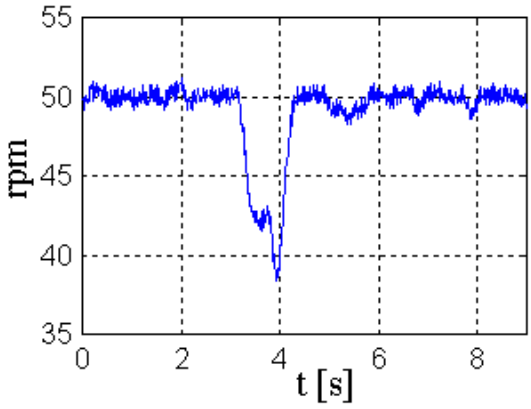

Figure 15: Response to a step torque disturbance

CONCLUSIONS

The possibility of using a heavy duty pneumatic motor to develop a servomotor for low velocity, high torque applications was analysed. It was developed a control layout technique based on a pressure proportional valve, and it was found that linear control technique is not suitable to operate in the whole operating range if a pressure proportional valve is used as a control device. A solution involving variable integrative and proportional gain was found, and the system shows satisfactory response time to step reference change and to torque disturbance. Flow rate control exerted by modulating valves showed to be a valuable alternative control technique. The performance obtained with the two techniques are comparable.

The system could hence be a possible alternative to hydraulic or electric solution when dynamic response is not a major issue, while easiness of installation and maintenance are more relevant requirements.

REFERENCES

[1] Mauro, S., Scarzella, C., (2010), Parallel mechanism for precision sun tracking, , ASME 2010 10th Biennial Conference on Engineering Systems Design and Analysis, ESDA2010, 2, pp. 17-22. DOI: 10.1115/ESDA2010-24100

[2] Battezzato, A., Mauro, S., Scarzella, C., (2012), Developing a parallel kinematic solar tracker for HCPV, ASME 2012 11th Biennial Conference on Engineering Systems Design and Analysis, ESDA 2012, 2, pp. 459-464. DOI: 10.1115/ESDA2012-82193

[3] Mauro, S., Battezzato, A., Biondi, G. and Scarzella, C. (2015), Design and test of a parallel kinematic solar tracker, Advances in Mechanical Engineering, December 2015 7, doi:10.1177/1687814015618627

[4] Pastorelli, S., Battezzato, A., 2009, "Singularity analysis of a 3 degrees-of-freedom parallel manipulator" Proceedings of the 5th International Workshop on Computational Kinematics, 2009, 331-340

[5] Mauro, S., Gastaldi, L., Pastorelli, S., and Sorli, M., (2016), Dynamic Flight Simulation with a 3 d.o.f. Parallel Platform, International Journal of Applied Engineering Research, Volume 11, Number 18 (2016) pp. 9436-9442

[6] Gastaldi, L., Pastorelli, S. and Sorli, M. (2016) Static and Dynamic Experimental Investigation of a Pneumatic Open Loop Proportional Valve, Experimental Techniques, DOI 10.1007/s40799-016-0142-5

[7] Gastaldi, L., Pastorelli, S., Caramella, M. and Dimanico, U. Indoor motion analysis of a subject wearing prosthesis for adaptive snowboarding, (2011) WIT Transactions on Biomedicine and Health 15, pp. 361-372.

[8] Sacco, K., Cauda, F., D'agata, F., Duca, S., Zettin, M., Virgilio, R., Nascimbeni, A., Belforte, G., Eula, G., Gastaldi, L., Appendino, S. and Geminiani, G. (2011) A combined robotic and cognitive training for locomotor rehabilitation: Evidences of cerebral functional reorganization in two chronic traumatic brain injured patients. Frontiers in Human Neuroscience, 5, art.n. 146, pp1-9

[9] Jacazio, G. and Gastaldi, L. (2010), An autonomous pneumotronic system for enhancing the braking capability of long freight trains,Proceedings of the ASME Dynamic Systems and Control Conference, DSCC2009 (PART B), pp. 1745-1752

[10] Mauro, S., Pastorelli, S. and Mohtar,T. (2014), Sensitivity Analysis of the Transmission Chain of a Horizontal Machining Tool Axis to Design and Control Parameters, Advances in Mechanical Engineering, January-December 2014 6: 169064, 2014, doi:10.1155/2014/169064

[11] Mauro, S., Pastorelli, S. and Johnston, E. (2015), Influence of controller parameters on the life of ball screw feed drives, Advances in Mechanical

Engineering, August 2015, 2015, doi:10.1177/1687814015599728

[12] Jacazio, G., Gastaldi, L. (2016) Robust pressure control improves the performance of redundant fly-by-wire hydraulic actuators. International Journal of Applied Engineering Research, 11(15), pp. 8590-8597

[13] Mattiazzo, G., Mauro, S., Guinzio, P.S., 2009, "A tensioner simulator for use in a pipelaying design tool", Mechatronics, 19 (8), pp. 1280-1285, doi: 10.1016/j.mechatronics.2009.08.004

[14] Sorli, M. and Gastaldi, L., (2009), Thermic influence on the dynamics of pneumatic servosystems, Journal of Dynamic Systems, Measurement and Control 131(2): 1-5.

[15] Lee, L. W., & Li, I. H. (2012). Wavelet-based adaptive sliding-mode control with H∞ tracking performance for pneumatic servo system position tracking control. IET control theory & applications, 6(11), 1699-1714.

[16] Yao, N. (2014). Sliding Model Control and its Application to Pneumatic Position Servo System. In Applied Mechanics and Materials (Vol. 473, pp. 259-262). Trans Tech Publications.

[17] Shang, C., Tao, G., & Meng, D. (2016). Adaptive robust trajectory tracking control of a parallel manipulator driven by pneumatic cylinders. Advances in Mechanical Engineering, 8(4), 1687814016641914.

[18] B.W. Mc Donell, J.E. Bobrow, "Modeling identification and control of a pneumatic actuated, force controllable, robot", IEEE Transaction on Robotics and Automation, l4(5), pp. 732-742 , 1998

[19] G. Mattiazzo, S. Mauro, T. Raparelli, M. Velardocchia, "Control of a Six Axis pneumatic Robot", J. Of Robotic Systems, Vol. 18, N° 8, pp. 363-378 , Aug. 2002

[20] Núñez, A. F., Veiga, F. F., Gonçalves, M. M., Teixeira, F. P., Horn, A. C., Estrada, E. S. D., & Botelho, S. S. C. (2013, March). A Pneumatic Robotic System for Inspection of Underground Electrical Conduit. In Computing and Automation for Offshore Shipbuilding (NAVCOMP), 2013 Symposium on (pp. 57-62). IEEE.

[21] Comber, D. B., Cardona, D., Webster III, R. J., & Barth, E. J. (2012). Precision pneumatic robot for MRI-guided neurosurgery. ASME J. Med. Dev, 6(1), 017587.

[22] Sorli M., Figliolini G., Pastorelli S., Rea P. (2005) Experimental identification and validation of a pneumatic positioning servo-system. Power Transmission and Motion Control, PTMC 2005, pp. 365-378.

[23] Belforte G., Mauro S., Mattiazzo S., (2004), A method for increasing the dynamic performance of pneumatic servosystems with digital valves, Mechatronics, Vol. 14, Issue 10, December 2004, Pages 1105-1120, DOI: 10.1016/j.mechatronics.2004.06.006